Available online at www.sciencedirect.com
ScienceDirect
Trans. Nonferrous Met. Soc. China 22(2012) 2855−2862
Transactions of Nonferrous Metals Society of China
www.tnmsc.cn

Electrodeposition of Ir on platinum in NaCl−KCl molten salt

QIAN Jian-gang, ZHAO Tian

School of Chemistry and Environment, Beihang University, Beijing 100191, China

Received 22 September 2011; accepted 7 January 2012

Abstract: The reduction mechanism of Ir in the NaCl−KCl−$IrCl_3$ molten salt was investigated by cyclic voltammetry and chronopotentiometry, and Ir film was deposited effectively on platinum in potentiostatic mode. The morphology and constitution of Ir film were examined by scanning electron microscopy (SEM), energy dispersive spectroscopy (EDS) and X-ray diffraction (XRD). It is found that the reduction mechanism of Ir(III) is a three-electron step and electro reaction is a reversible diffusion controlled process; the diffusion coefficients of Ir(III) at 1083, 1113, 1143 and 1183 K are 1.56×10^{-4}, 2.23×10^{-4}, 2.77×10^{-4} and 4.40×10^{-4} cm^2/s, respectively, while the activation energy of the electrode reaction is 102.95 kJ/mol. The compacted Ir film reveals that the applied potential greatly affects the deposition of Ir, the thickness of Ir film deposited at the potential of reduction peak is the highest, the temperature of the molten salt also exerts an influence on deposition, the film formed at a lower temperature is thinner, but more micropores would occur on film when the temperature went too high.

Key words: Ir; NaCl−KCl molten salt; NaCl−KCl−$IrCl_3$ molten salt; electrodeposition; reduction mechanism; electrode reaction; activation energy; micro-pores

1 Introduction

Iridium has a high melting point (2713 K) and is chemically stable at a ultra-high temperature. Iridium possessing a property to be a good diffusion barrier to carbon and oxygen can work in low-oxidation atmosphere and high rate of airflow scour at 2473 K for a long time [1−3]. Therefore, iridium is often used as the protective film for structural material against extreme environments, such as turbine engine, rocket thruster and thermal generator, and is the most promising candidate in the aeronautic, astronautic, navigation and civilian fields [4−6].

Ir film has been prepared by many different deposition methods, including CVD [7−9], magnetron sputtering (MS) [3,4], double glow plasma (DGP) [2,10], pulsed laser deposition (PLD) [11], laser-induced chemical decomposition (LICD) [12] and electroformed deposition (ED) [13] etc.

Compared with other methods of forming Ir film, molten salt has a lot of advantages. For example, there is no water in the molten salt, and the potential of by-reaction of anode is more positive while the potential of by-reaction of cathode is more negative than that of water. So, it provides not only a quicker and more economical way to form Ir film, but also with no distinct damage to the substrate during the deposition. As a result, many pure metals and functional materials which cannot be deposited in water can be deposited.

Some work has been reported so far about the electrodeposition of Ir film in the molten salt. WITHERS and RITT [14] reported the preparation of Ir films in constant current mode and pulse mode in cyanide molten salt. But cyanide is harmful to the environment and thus prohibits the extensive use of the process. SALTYKOVA and PORTNYAGIN [15,16] studied the possibility of formation of Ir−Ru alloy in constant current electrodeposition in the chloride molten salt and measured the composition of the alloy at different temperatures.

In this study, by means of cyclic voltammetry and chronopotentiometry, the chemical behavior of Ir(III)/Ir(0) on a Pt working electrode in the NaCl−KCl−$IrCl_3$ molten salt was investigated. The influence of technological parameters on Ir film was discussed; the composition and structure of the Ir film was examined by scanning electron microscopy (SEM), energy dispersive spectroscopy (EDS) and X-ray diffraction (XRD).

Corresponding author: ZHAO Tian; Tel: +86-15010033057; E-mail: zhaotian63@sina.com
DOI: 10.1016/S1003-6326(11)61542-2

2 Experimental

In the field of the molten salt, the eutectic mixture NaCl−KCl is considered a "standard molten medium" for many processes and is widely used in the separation, purification and synthesis for a wide range of metals [17]. Consequently, the eutectic mixture of NaCl−KCl molten salt (with a molar ratio of 1:1) was chosen as the solvent to study the iridium electrochemical behavior. Equimolar NaCl−KCl mixture (a total mass of the salt is 30 g) was placed in the corundum crucible, which was set as the electrochemical reaction cell. Then the cell was sealed and put in a self-made resistance furnace. The salt in the cell was heated slowly up to 573 K under vacuum for about 12 h, while dry Ar was passed into the furnace to maintain an inert gas atmosphere [15]. The schematic diagram of molten salt furnace is shown in Fig. 1.

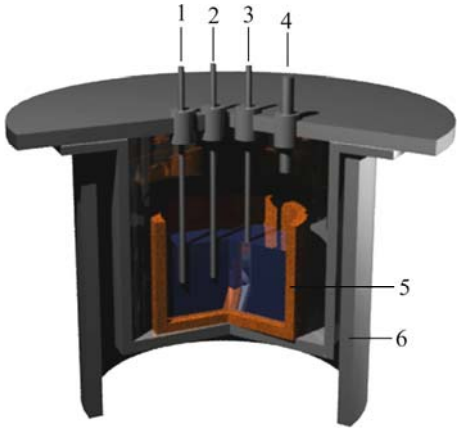

Fig. 1 Schematic diagram of self-made molten salt furnace: 1—Counter electrode; 2—Working electrode; 3—Reference electrode; 4—Vent; 5—Corundum crucible; 6—Self-made resistance furnace

The electrochemical experiments were performed with a three-electrode cell. The conventional inert metal-platinum as the working electrode leads a dominate position in the research of the mechanism of electrodeposition of metal ions [18,19]. And a platinum wire (99.95% in purity, 1 mm in diameter) was used as the working electrode and the area of the platinum wire was controlled by the immersion depth (typically, 6 mm). An iridium plate with a surface area of 15 mm×20 mm was used as the counter electrode while the reference electrode was another platinum wire (99.95% in purity, 0.5 mm in diameter). In order to increase the binding force between the working electrode and the iridium film during the process of the electrodeposition, the working electrode had been thoroughly polished with 1500# SiC paper, and then ultrasonically cleaned in a NaOH solution (5% of mass fraction). Before the process of the electrodeposition, all the electrodes were cleaned by deionized water and then oven-dried.

The whole electrochemical study was performed on a chi660d electrochemical workstation, while the temperature was measured using an automatic temperature control system of the self-made resistance furnace with an accuracy of ±1 K. The composition and structure of the deposit were analyzed with Japan S−530 scanning electron microscope equipped with energy dispersive spectroscope, Quanta 250 environmental scanning electron microscope and X-ray diffraction.

3 Results and discussion

3.1 Electrochemical behavior of Ir(III)/Ir(0) in NaCl−KCl molten salt based on cyclic voltammogram

The electrochemical behavior of Ir(III)/Ir(0) has been studied by cyclic voltammogram in NaCl−KCl molten salt. Figure 2 shows a typical cyclic voltammogram (CV) of the Pt wire working electrode immersed in molten NaCl−KCl of 1113 K; the sweep rate was 200 mV/s.

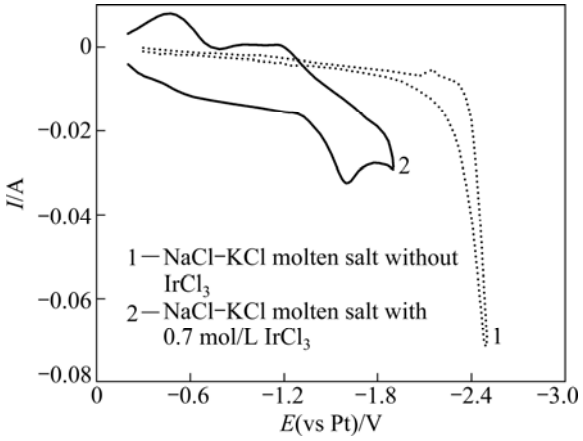

Fig. 2 Cyclic voltammogram obtained from Pt working electrodes in molten NaCl−KCl of 1113 K at scan rate of 200 mV/s

The curve 1 in Fig. 2 shows that a strong cathodic peak occurs around −2.0 V, which associated with alkali metal deposition and dissolution reactions. When $IrCl_3$ was added into the molten salt, the CV curve changed significantly, as presented in curve 2. Curve 2 exhibits the presence of one reversible wave, observed at −1.6 V. By comparing curve 2 with curve 1, the reduction peak at −1.6 V was related to the reduction of Ir(III)→Ir(0).

At the potential ranging from −0.2 V to −1.9 V in NaCl−KCl−$IrCl_3$, a series of voltammograms recorded with a Pt working electrode in the scan rate range of 200 mV/s to 400 mV/s are shown in Fig. 3. Based on the

method for determining the reversible reaction according to CV [20], the reaction can be concluded as the reversible reaction when the reduction peak potential does not vary with the sweep rate. It can be seen from Fig. 3 that the current intensity of cathodic peak kept increasing as the sweep rate rose gradually from 200 mV/s to 400 mV/s, while the reduction peak potential did not vary significantly. Therefore, it can be concluded that the reduction process of Ir(III)/Ir(0) is reversible.

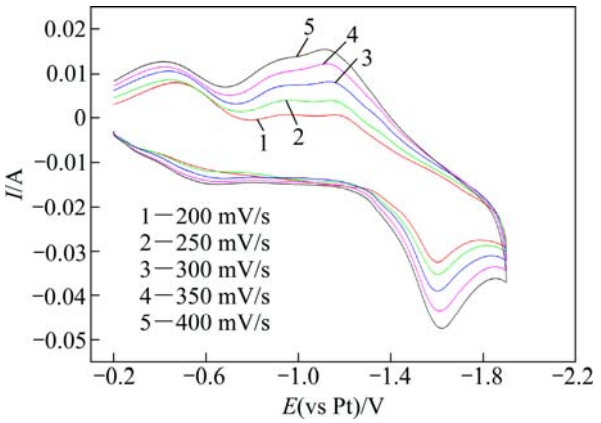

Fig. 3 Cyclic voltammograms obtained with Pt working electrode in NaCl−KCl−Ir_3($c_{Ir(III)}$=0.7 mol/L) at various scan rates (A =0.12 cm^2, T=1113 K)

According to BARD and FAULKNER [21], in the electrochemical reaction, the peak potential, the half peak potential and the number of the electrons transferred for the reaction follow the relation below:

$$E_p - E_{p/2} = -2.2RT/nF$$

where E_p is the peak potential; $E_{p/2}$ is the half peak potential; T is the operation temperature; n is the number of the electrons transferred in the reaction. In this experiment, based on the data of E_p and $E_{p/2}$ which had been got from the CV curve at different temperatures, the number of the electrons transferred of Ir(III)/Ir(0) was determined to be 3. So, the reduction mechanism of Ir(III) is considered to be a three-electron step:

$$Ir^{3+} + 3e^- = Ir$$

In the case of a diffusion controlled reversible electrochemical reaction, the corresponding physical variables conform to the Randle-Sevick equation [22，23], which indicates that the current of the reduction peak varies linearly with the square root of sweep rate:

$$I_{pc} = 0.4463A\left(\frac{n^3F^3}{RT}\right)^{1/2} D_{Ir(III)}^{1/2} c_{Ir(III)} v^{1/2} I$$

where I_{pc}, $c_{Ir(III)}$, $D_{Ir(III)}$, v and A represent the current of the cathodic peak, the concentration of Ir(III) in the molten salt, the diffusion coefficient for Ir(III), the sweep rate and the surface area of the working electrode, respectively.

Figure 4 shows the relationship between I_{pc} and $v^{1/2}$ in the NaCl−KCl−$IrCl_3$ molten salt at different temperatures. It can been seen clearly from Fig. 4 that a linear variation of I_{pc} with $v^{1/2}$ was observed on the platinum electrode in the temperature range of 1083−1183 K, indicating that the electrode process is diffusion controlled.

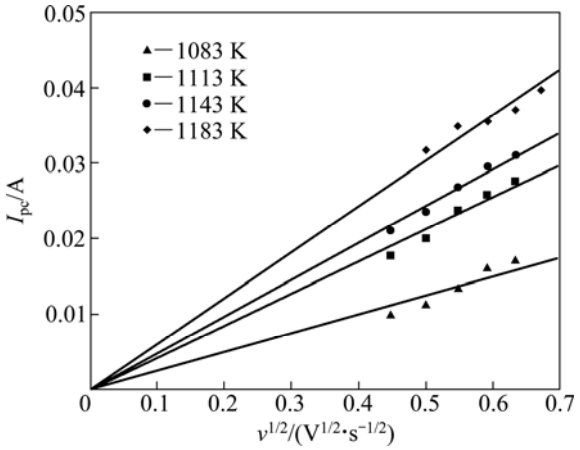

Fig. 4 Randle-Sevick plots of reduction peak I_{pc} vs $v^{1/2}$ for Ir(III) reduction on Pt in NaCl−KCl−$IrCl_3$ at various melt temperatures ($c_{Ir(III)}$=0.7 mol/L, A=0.12 cm^2)

3.2 Chronopotentiometry of Ir(III) in NaCl−KCl molten salt

Chronopotentiometry was carried out on a Pt working electrode in the NaCl−KCl−$IrCl_3$ over the same temperature range (from 1083 K to 1183 K) to further investigate the reduction mechanism of Ir(III). Typical chronopotentiograms were obtained at 1083 K, and presented in Fig. 5. Figure 5 reveals that the transition time τ decreased with the rising of current intensity. In the plots given, the potential plateau observed at around −1.6 V was associated with the reduction of Ir(III). To confirm the reduction mechanism of Ir(III), the Nernst equation applied in the reversible reaction was carried out [20]:

$$\left|E_{\tau/4} - E_{3\tau/4}\right| = 0.16T/n$$

wherein $E_{\tau/4}$ is the 1/4 wave potential value; $E_{3\tau/4}$ is 3/4 of the value; T and τ represent the temperature and the transition time, respectively; n is the number of electrons transferred during the reaction. The results obtained from Fig. 5 can calculate the number of electrons transferred in the reaction to be about 3.0, which coincides with the value determined by cyclic voltammograms above. Consequently, the reaction mechanism of Ir(III) is a three-electron step.

When the reaction is a diffusion controlled process, the relationship between the current I and transition time τ conformed to the Sand equation [22]:

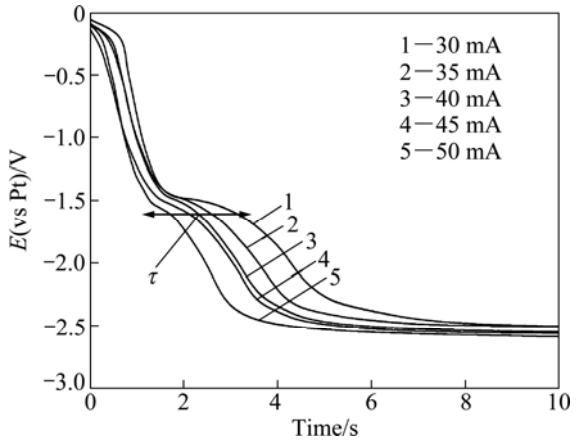

Fig. 5 Chronopotentiograms obtained at various applied current on Pt electrode in NaCl−KCl−$IrCl_3$ at 1083 K ($c_{Ir(III)}$=0.7 mol/L, A=0.12 cm^2)

$$I=\frac{nFAc_{Ir(IIII)}(\pi D_{Ir(III)})^{1/2}}{2}\tau^{-1/2}$$

where I, τ, $c_{Ir(III)}$ and $D_{Ir(III)}$ represent the current, the transition time, the concentration of Ir(III) and the diffusion coefficient of Ir(III), respectively; n is the number of the electrons transferred in the reaction. The plots of I vs $\tau^{-1/2}$ at different temperatures in the NaCl−KCl−$IrCl_3$ are presented in Fig. 6. An excellent linear relationship between I and $\tau^{-1/2}$ is obtained on a Pt electrode at different temperatures, indicating that the electrode reaction of Ir(III)→Ir(0) is a diffusion controlled process.

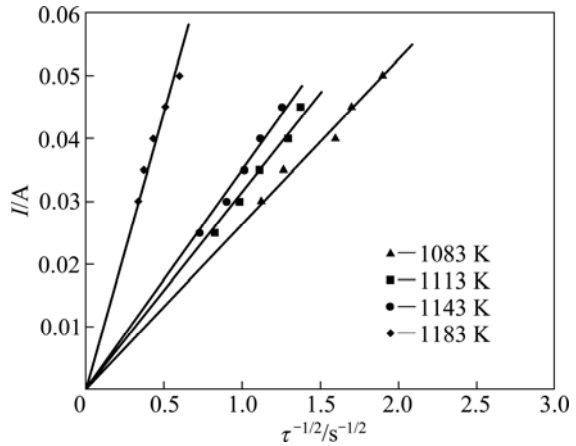

Fig. 6 Relationship between I and $\tau^{-1/2}$ at different temperatures in NaCl−KCl−$IrCl_3$ (working electrode: Pt; $c_{Ir(III)}$=0.7 mol/L; A=0.12 cm^2)

According to the Sand equation, the diffusion coefficient of Ir(III) at each temperature given in the plot in the NaCl−KCl−$IrCl_3$ can be calculated as listed in Table 1.

It can be concluded that the diffusion coefficient of Ir(III) is positively related to temperature. From the result obtained above, the reaction is a diffusion controlled process. Therefore, the relationship between the diffusion coefficient $D_{Ir(III)}$ and temperature T follows the Arrhenius law[25]:

Table 1 Experimental values of $D_{Ir(III)}$ of Ir(III) obtained on a Pt electrode in NaCl−KCl−$IrCl_3$ at different temperatures

T/K	$D_{Ir(III)}$/(10^4 $cm^2\cdot s^{-1}$)
1083	1.56
1113	2.23
1143	2.77
1183	4.40

$$D_{Ir(III)}=D_0\exp(-\frac{E_a}{RT})$$

where $D_{Ir(III)}$, D_0, E_a and T represent the diffusion coefficient of Ir(III), the pre-exponential factor, the activation energy and temperature, respectively. Figure 7 presents the relationship between $\ln D_{Ir(III)}$ and the reciprocal of temperature T^{-1}. A straight line was obtained as follows:

$$\ln D_{Ir(III)}=2.71-12383T^{-1}$$

Associated with Arrhenius law, the activation energy of Ir(III) in the NaCl−KCl−$IrCl_3$ can be calculated to be E_a=102.95 kJ/mol.

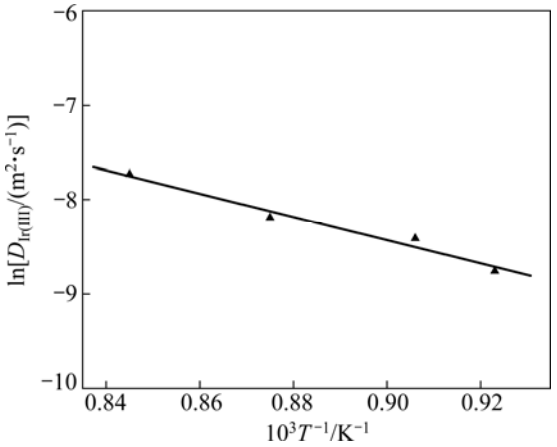

Fig. 7 Relationship between diffusion coefficient $D_{Ir(III)}$ and temperature T in NaCl−KCl−$IrCl_3$ (working electrode: Pt, $c_{Ir(III)}$=0.7 mol/L; A=0.12 cm^2)

3.3 Electrodeposition of Ir film in potentiostatic mode

The electrodeposition experiments to prepare Ir film were carried out potentiostatically in the NaCl−KCl−$IrCl_3$ molten salt. From the CV measurements in Fig. 2, the electrodeposition potential of forming Ir films was assumed to be about −1.6 V vs Pt. A series potentials of around −1.6 V were chosen to further investigate the influence of potential on the morphology of the deposited Ir film. Figure 8 presents the surface morphologies of Ir film formed under the potentials of

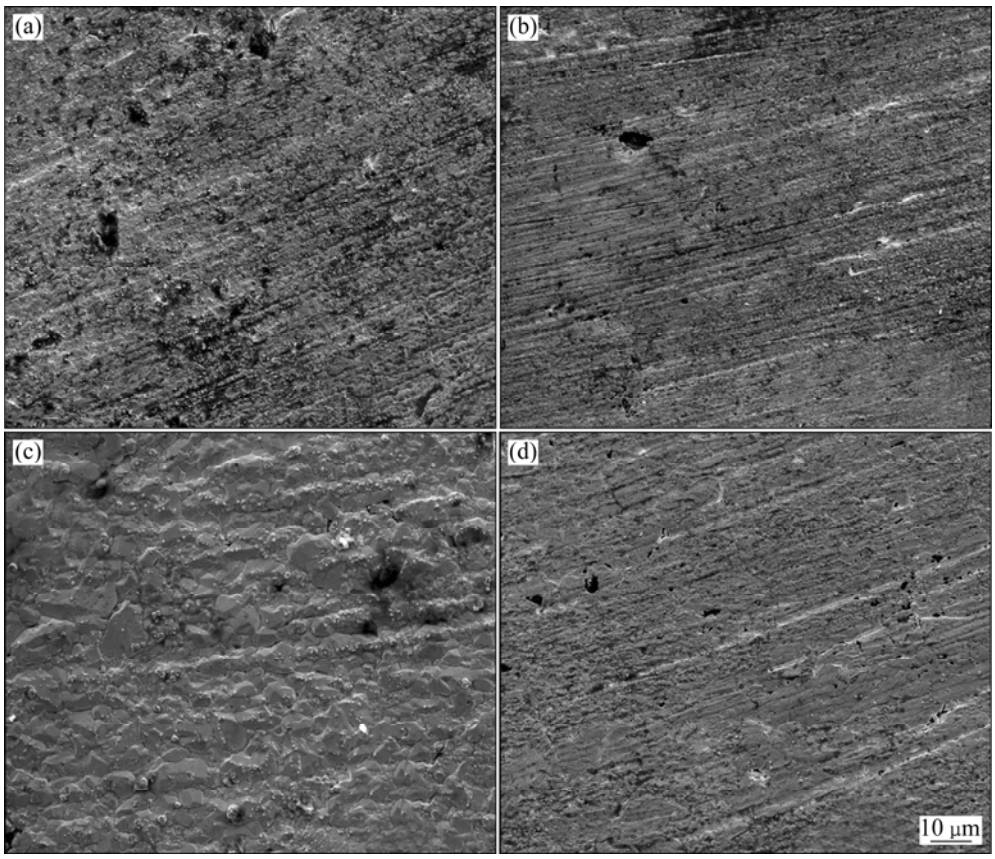

Fig. 8 SEM images of Ir films deposited in NaCl−KCl−$IrCl_3$ of 1113 K at various deposition potentials for 30 min: (a) −1.4 V; (b) −1.5 V; (c) −1.6 V; (d) −1.7 V

−1.4, −1.5, −1.6 and −1.7 V, respectively. All of the deposition time was 30 min. The Ir films produced at −1.4, −1.5 and −1.7 V were so thin that the substrate can still be seen. EDS analysis of the electrodeposition revealed that the mass fractions of the Ir in the films deposited at −1.4, −1.5, −1.6 and −1.7 V were 73.7%, 84.2%, 100.0% and 55.1%, respectively. Furthermore, the highest value was the film formed at −1.6 V. Therefore, the optimized electrodeposition potential is selected as the reduction peak potential.

For an applied potential of −1.6 V and an electrodeposition time of 30 min, the surface morphologies of Ir films formed at 1083, 1113 and 1163 K are shown in Fig. 9. It can be seen from Fig. 9 that when the electrodeposition temperature was 1083 K (Fig. 9(a)), the scratches of the substrate can be seen and the mass fraction of Ir in the film was as low as 33.5% according to EDS, which indicates that the film is still thin. The fact lies in that when the molten salt had a low temperature, the viscosity of the molten salt was high enough to lower the electro activity of Ir(III), so that the nucleation sites were reduced in the salt. When the temperature increased to 1113 K (Fig. 9(b)), the surface morphology changed significantly and the mass fraction of Ir increased to 100.0%. This was due to the fact that with increasing diffusion rate of the Ir(III), more active Ir(III) sites were produced at higher temperature[22]. Therefore, the deposition amount of Ir was raised. When the temperature, however, was increased to 1163 K, the mass fraction of Ir was 84.8%, a little lower than that at 1113 K, and some micropores appeared on the surface of the deposited film seen in Fig. 9(c). This was probably due to the fact that both the activity of molten salt and the by-reaction, such as alkali metal deposition and dissolution reaction, increased at ultra-high temperature of the molten salt resulting in the micropores occurring in the films. From these series experiments, the optimized temperature for electrodeposition of Ir was determined at 1113 K.

Figure 10 shows the surface morphologies of the Ir films obtained with a deposition time of 1, 5, 20 and 30 min, respectively at 1113 K and an applied potential of −1.6 V. Some Ir particles formed on the substrate when the deposition time was 1 min; more Ir particles formed on the substrate as the deposition time extended to 5 min; the substrate was almost fully covered by the Ir particles when the deposition time extended to 20 min; finally, a dense and compact Ir film was formed on the substrate when deposition time was 30 min. The films were further analyzed by XRD to investigate the phase and the results

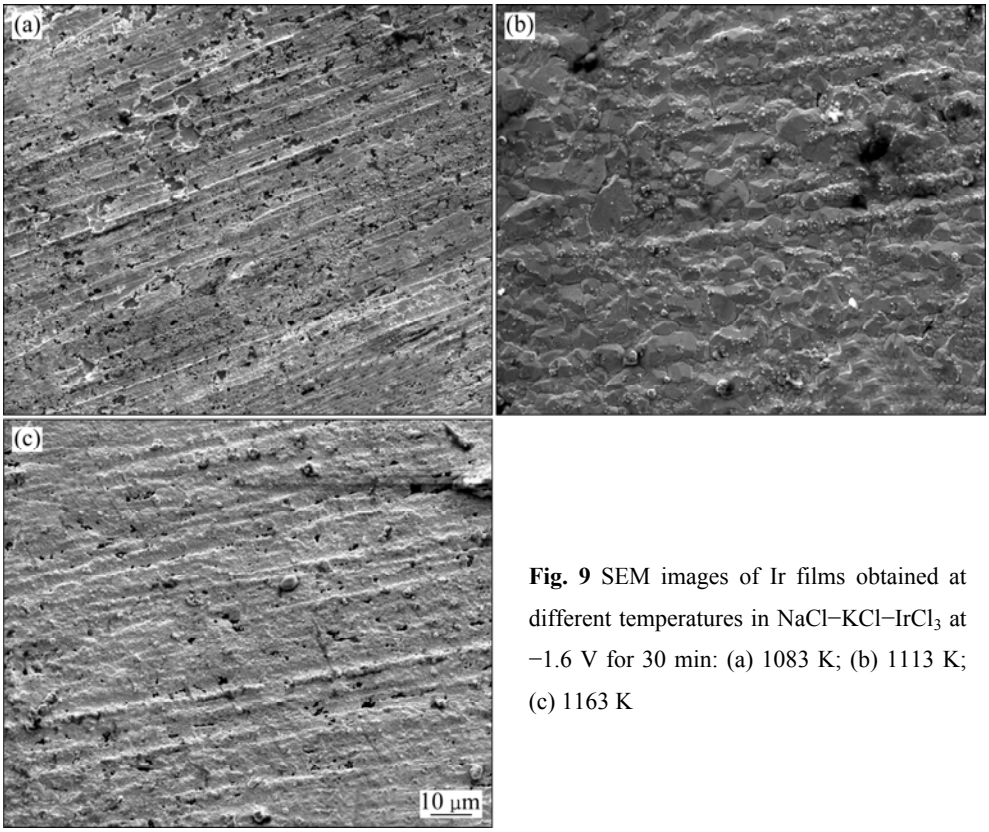

Fig. 9 SEM images of Ir films obtained at different temperatures in NaCl−KCl−$IrCl_3$ at −1.6 V for 30 min: (a) 1083 K; (b) 1113 K; (c) 1163 K

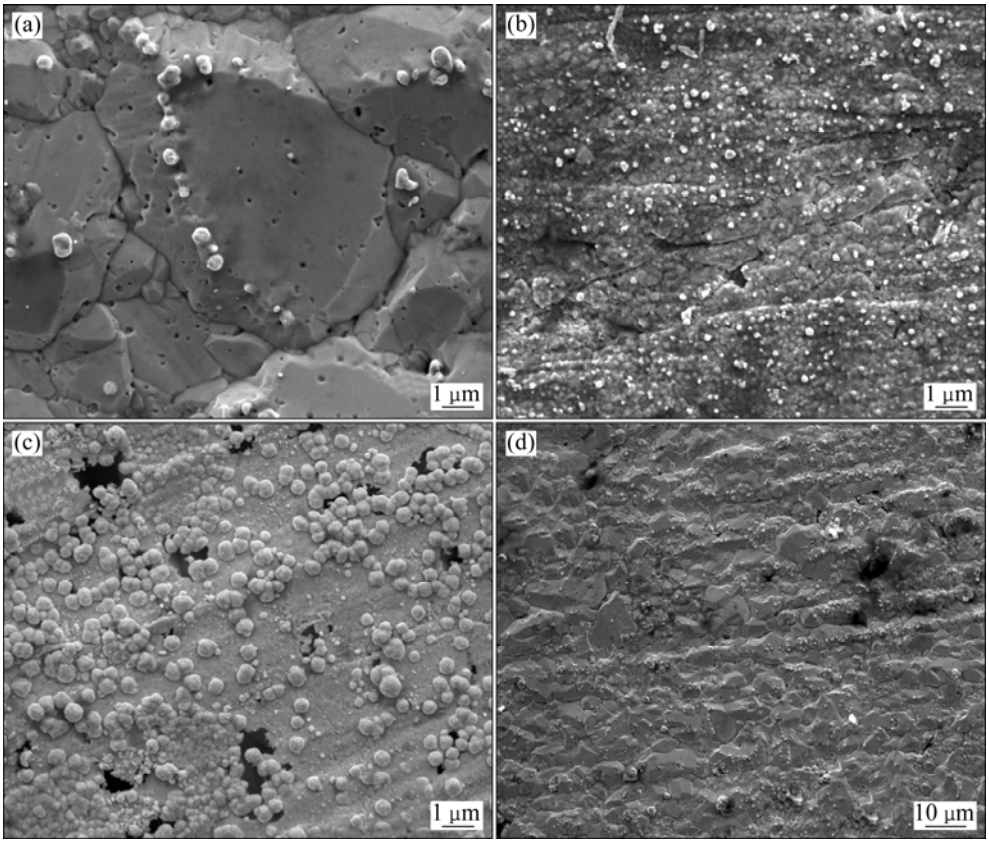

Fig. 10 SEM images of Ir films obtained in NaCl−KCl−$IrCl_3$ at −1.6 V of different deposition time: (a) 1 min; (b) 5 min; (c) 20 min; (d) 30 min

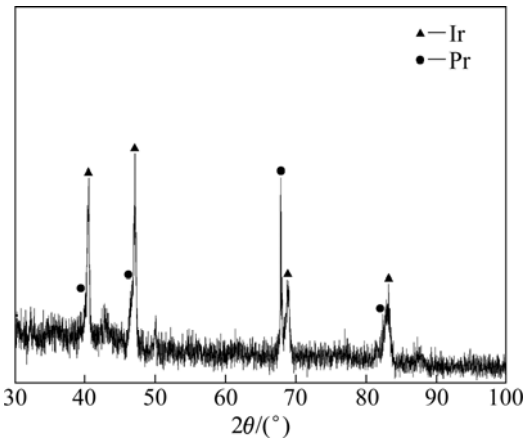

Fig. 11 XRD pattern of Ir film obtained with deposition time of 30 min

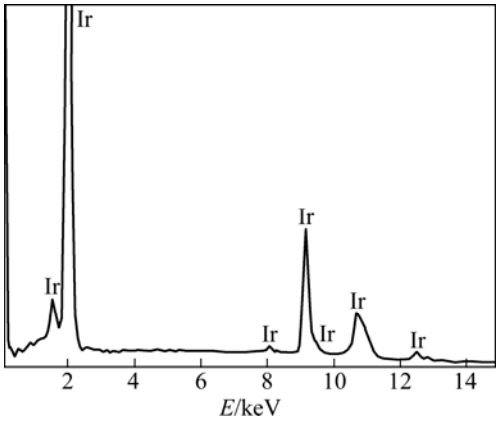

Fig. 12 EDS analysis of Ir film obtained with deposition time of 30 min

showed that pure Ir was contained in the films. Figures 11 and 12 show the typical XRD and EDS patterns obtained with a deposition time of 30 min.

4 Conclusions

1) According to cyclic voltammogram and chronopotentiometry, the reduction mechanism of Ir(III) is a three-electron step in the NaCl−KCl−$IrCl_3$.

2) The electrochemical reaction of Ir(III)→Ir(0) is a reversible diffusion controlled process; the diffusion coefficients of Ir at 1083, 1113, 1143 and 1183 K are 1.56×10^{-4}, 2.23×10^{-4}, 2.77×10^{-4} and 4.40×10^{-4} cm^2/s, respectively.

3) The activation energy of Ir(III) is 102.95 kJ/mol. The compacted Ir film reveals that the applied potential greatly affects the deposition of Ir, and the films deposited at the potential of reduction peak is the thickest.

4) The temperature of the molten salt also affects the deposition. The films deposited at lower temperature were thinner, but too many micropores would occur on the films at ultra-high temperature; the mass fraction of Ir would increase with extension of the deposition time.

References

[1] High-temperature oxidation-resistant coatings-coating for protection from oxidation of superalloys refractory metals, and graphite [M]. Washington, D.C: National Academy of Sciences/National Academy of Engineering, 1970.

[2] WU W P, LIN X, CHEN Z F, CHEN Z, CONG X N, XU T Z, QIU J L. Microstructural characterization and mechanical property of iridium coating produced by double glow plasma [J]. Plasma Chem Plasma Process, doi:10.1007/s11090- 011−9293-4.

[3] MUMATAZ K, ECHIGOYA J, HIRAI T, SHINDO Y. Magnetron sputtered iridium coatings on carbon structural materials [J]. Mater Sci Eng A, 1993, 167: 187−195.

[4] KHAKANI M A, CHAKER M, le DROGOFF B. Iridium thin films deposited by radiofrequency magnetron sputtering [J]. J Vac Sci Technol A, 1998, 16: 885−888.

[5] REED B D, DICKERSON R. Testing of electroformed deposited iridium/powder metallurgy rhenium rockets [M]. Washington DC: National Aeronautics and Space Administration, 1995: 1−9.

[6] Ultramet-Advanced Materials Solutions. Propulsion system components, liquid rocket engines [EB/OL]. [2011−09−10]. http://www.ultramet.com/propulsionsystem components liquid rocket.html.

[7] GARCIA J R V, GOTO T. Chemical vapor deposition of iridium, platinum, rhodium and palladium [J]. Mater Trans, 2003, 44: 1717−1728.

[8] HAMDEN-SMITH M J, KODAS T T. Chemical vapor deposition of metals: Part 1. An overview of CVD processes [J]. Chem Vap Deposition, 1995, 1(1): 8−23.

[9] KODAS T T, HAMDEN-SMITH M J. The chemistry of metal CVD, VCH [M]. Germany: Weinheim, 1994: 170−177.

[10] WANG L B, CHEN Z F, ZHANG Y, WU W P. Ir coating prepared on Nb substrate by double glow plasma [J]. Int J Refract Met Hard Mater, 2009, 27: 590−594.

[11] GONG Y S, WANG C B, SHEN Q, ZHANG L M. Low-temperature deposition of Iridium thin films by pulsed laser deposition [J]. Vacuum, 2008, 82: 594−598.

[12] SNELL L, NELSOM A, MOLIAN P. A novel laser technique for oxidation-resistant coating of carbon-carbon composite [J]. Carbon, 2001, 39: 991−999.

[13] ETENKO A, MCKECHNIE T, SHCHETKOYSKIY A, SMIRNOV A. Oxidation-protective iridium and iridium-rhodium coatings produced by electrodeposition from molten salts [J]. ECS Trans, 2007, 3: 151−157.

[14] WITHERS J C, RITT P E. Iridium plating and its high temperature oxidation resistance [C]//Technical Proceedings of the American Electroplaters Society. Pennsylvania: University of Pennsylvanis, 1957, 44: 124−129.

[15] SALTYKOVA N A, PORTNYAGIN O V. Electrodeposition of Ir−Ru alloys from chloride melts: Steady-state potentials and cathodic processes [J]. Russian Journal of Electrochemistry, 2000, 36(7): 784−788.

[16] SALTYKOVA N A, PORTNYAGIN O V. Electrodeposition of irdium-ruthenium alloys from chloride melts: The structure of the deposits [J]. Russian Journal of Electrochemistry, 2001, 37(9): 924−930.

[17] GEORGE W. Handbook of solvents [M]. 1st ed. Michigan: Chem Tec, 2001: 622−637.

[18] DUAN Shu-zhen, DUDLEY P, INMAN D. Voltammetric studies of iron in molten $MgCl_2$+NaCl+KCl: Part I. The reduction of Fe(II) [J].

J Electroanal Chem, 1982, 142: 215−228.
[19] ALEX L, MICHAEL Z. Electrodeposition of iron(II) on platinum in chloride melts at 700−750 °C [J]. Electrochimica Acta, 2009, 54: 1904−1908.
[20] RERNMUTH W H. Theory of stationary electrode polarography [J]. Anal Chem, 1961, 33: 1793−1794.
[21] BARD A J, FAULKNER L R. Electrochemical methods, fundamentals and applications [M]. New York: Wiley, 1980.
[22] SCHIFFRIN D J. Theory of cyclic voltammetry for reversible electrodeposition of insoluble products [J]. J Electroanal Chem, 1986, 201: 199−203.
[23] BERZINS T, DELAHAY P. Oscillographic polarographic waves for the reversible deposition of metals on solid electrodes [J]. J Am Chem Soc, 1953, 75: 555−559.
[24] BARD A J, FAULKNER L R. Electrochemical methods: Fundamentls and applications [M]. 2nd ed. New York: John Wiley & Sons Inc, 2000.
[25] GROULT H, GHALLALI H E, BARHOUN A. Preparation of Co−Sn alloys by electroreduction of Co(II) and Sn(II) in molten LiCl−KCl [J]. Electrochimica Acta, 2010, 55: 1926−1932.

NaCl−KCl−$IrCl_3$ 熔盐体系中电沉积 Ir 层的机理

钱建刚，赵 天

北京航空航天大学 化学与环境学院，北京 100191

摘 要：在 NaCl−KCl−$IrCl_3$ 熔盐体系中利用循环伏安法和计时电位法研究 Ir 的沉积机理并通过恒电位法在 Pt 基体上制备出 Ir 层。利用扫描电子、显微镜(SEM)能谱仪(EDS)和 X 射线衍射仪(XRD)对 Ir 层的表面形貌和成分进行分析。结果表明：在 NaCl−KCl−$IrCl_3$ 熔盐体系中 Ir 的电沉积过程为 Ir^{3+}获得 3 个电子一步沉积为 Ir，并且 Ir(Ⅲ)→Ir(0) 的电极反应过程为可逆扩散控制过程；在 1063、1113、1143 和 1183 K 下 Ir(Ⅲ)离子的扩散系数分别为 0.60×10^{-4}、1.23×10^{-4}、2.77×10^{-4} 和 4.40×10^{-4} cm^2/s，Ir(Ⅲ)在 NaCl−KCl−$IrCl_3$ 熔盐体系中电极反应的活化能 E_a=162.61kJ/mol；沉积电位对所获得的 Ir 层的形貌有较大影响，其中在峰值电位下所获得的 Ir 层较厚；熔盐温度对电沉积 Ir 层的形貌也有较大影响，在较低熔盐温度下获得的 Ir 层较薄，较高熔盐温度获得的 Ir 层的孔隙较多。

关键词：Ir；NaCl−KCl 熔盐；NaCl−KCl−$IrCl_3$ 熔盐；电沉积；还原机理；电极反应；活化能；微孔

(Edited by YANG Hua)